EUROPHYSICS LETTERS 15 August 2005

Europhys. Lett., **71** (4), pp. 618–624 (2005)
DOI: 10.1209/epl/i2005-10133-0

Strain softening and hardening of amorphous polymers: Atomistic simulation of bulk mechanics and local dynamics

A. V. Lyulin[1](*), B. Vorselaars[1], M. A. Mazo[2], N. K. Balabaev[3] and M. A. J. Michels[1]

[1] *Group Polymer Physics, Eindhoven Polymer Laboratories and Dutch Polymer Institute - Technische Universiteit Eindhoven P.O. Box 513, 5600 MB Eindhoven, The Netherlands*
[2] *Institute of Chemical Physics - Moscow 119991, Russia*
[3] *Institute of Mathematical Problems of Biology - Pushchino 142290, Russia*

received 4 April 2005; accepted in final form 24 June 2005

PACS. 62.20.Fe – Deformation and plasticity (including yield, ductility, and superplasticity).
PACS. 83.10.Mj – Molecular dynamics, Brownian dynamics.
PACS. 64.70.Pf – Glass transitions.

Abstract. – Molecular-dynamics (MD) simulations have been performed for two amorphous polymers with extremely different mechanical properties, atactic polystyrene (PS) and bisphenol A polycarbonate (PC), in the isotropic state and under load. The glass transition temperatures, Young moduli, yield stresses and strain-hardening moduli are calculated and compared to the experimental data. Both chemistry-specific and mode-coupling aspects of the segmental mobility in the isotropic case and under the uniaxial deformation have been identified. The mobility of the PS segments in the deformation direction is increased drastically beyond the yield point. A weaker increase is observed for PC.

The mechanisms of the segmental mobility of amorphous polymers in the glassy state pose a great challenge in soft-matter physics and are of high technological importance. The problem of establishing the nature of this mobility arises from the complex microstructure and from the time scales of structural relaxations that dominate the response of amorphous polymers. Understanding the connection between polymer chemical structure and bulk mechanical properties will open up ways of designing materials with extreme ultimate properties.

In recent years a number of major steps forward have been made among others through experimental micromechanical analysis [1], multi-level finite-element modelling [2], and simulation [3]. Tensile-testing experiments [4] reveal that polystyrene (PS) is brittle (*i.e.* there is only very little plastic deformation before failure occurs due to the crack formation) and polycarbonate (PC) is ductile (*i.e.* it can withstand significant strains before rupture). The plane strain fracture toughness (a measure of a material resistance to brittle fracture) is 0.7–1.1 MPa $\cdot\, m^{1/2}$ for PS and 2.2 MPa $\cdot\, m^{1/2}$ for PC [5]. On the other hand, on the microscopic

(*) E-mail: A.V.Lyulin@tue.nl

level it has proved possible [1] to measure the intrinsic large-deformation stress-strain behaviour, with the surprising result that PS is at that level far more ductile than PC. There exists an excellent correlation between the microscopically measured maximum extension ratio and the theoretical maximum extension ratio of a single strand in the polymer entanglement network [1]. It has recently been found [6] that by mechanical treatment PS and PC both become very ductile macroscopically and can be made to deform by shear yielding. However, the relaxation back to the original state is orders of magnitude faster for PS than for PC. Smit *et al.* [2] have performed multi-level modelling, with the microscopic elasto-viscoplastic constitutive equation as an input, with large-strain homogenisation of heterogeneous domains, and with a subsequent finite-element representation of the microstructure. They were able to predict the global mechanical behaviour of filled amorphous polymers under different loading conditions from their continuum-microscopic properties.

In [2, 6] both the origin and variety of the microscopic stress-strain behaviour, and the difference in relaxational properties between different amorphous polymers, are an open problem. The underlying mechanisms of this chemistry-specific difference between amorphous polymers remain unclear. Recently, universal behaviour has been found in different types of segmental mobility for a model amorphous polystyrene above and below the glass-transition temperature T_g [3]. In particular, the slowing-down of motion above T_g is in good agreement with the predictions of the mode-coupling theory (MCT) [7, 8].

The aims of the present study are to bring further insight via atomistic molecular-dynamics simulations into the role of the polymer structure and of the inter- and intramolecular interactions *vs.* the mechanical stress-strain behaviour. Such simulations in particular should allow us to separate the effects of chemistry-specific properties from generic physical mechanisms governing the mobility above and below T_g. We report the results of simulations for two mechanically very different glassy polymers —a typical brittle one, atactic polystyrene, and a typical ductile one, bisphenol A polycarbonate. We simulated the uniaxial deformation of both polymers to study the experimentally observed strain-softening and strain-hardening phenomena and to find possible links of these phenomena with the different mobilities on the segmental level.

The united-atom models of polymers are used in the present study; for PS the model is described in detail by Lyulin *et al.* [3]; for PC the force field of Hutnik *et al.* [9] is used. The simulation details are mentioned in [3]. In short, the *NPT* MD simulation has been performed for a model PS melt consisting of 1–8 polymer chains of $N_p = 80$–160 monomers each (molecular weight ≈ 8300–16600 Da, about one entanglement length) and its periodic images. The stereochemic configurations of the aromatic groups were generated at random so that the ratio of the number of *meso* to *racemic* dyads was near unity. 64 chains of $N_p = 10$ monomers (about one entanglement length, 64×10 system) and 8 chains of $N_p = 80$ monomers (about 8 entanglement lengths, 8×80 system) have been used for the PC melt. The leap-frog velocity Verlet algorithm [10] has been used to integrate the Newtonian equations of motion with the time step of $\Delta t = 4$ fs. The Berendsen *NPT* MD algorithm [10] has been used, with time constants $\tau_T = 0.5$ ps and $\tau_P = 1$ ps. Some runs have been performed using the collisional thermostat [11].

Glass transition. – First of all, the MD simulation was used in order to produce PS and PC in a glassy state. Both PS and PC polymer melts have been cooled down with a continuous cooling rate of 5×10^{-2} K/ps from the initial high-temperature liquid state at $T = 630$ K. Also step-wise cooling with steps down in temperature (about 10 K), followed by an equilibration of 20 ns has been performed, for a PS melt only. The temperature dependence of the specific volume at atmospheric pressure is shown in fig. 1. The specific volume decreases almost linearly with decreasing temperature at both high and low temperature. The clear

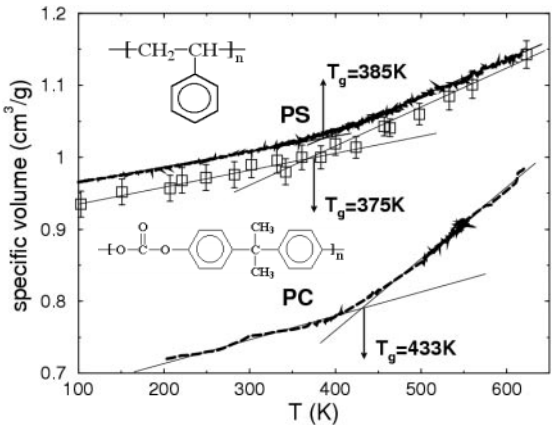

Fig. 1 – Temperature dependence of the specific volume for PS and PC produced with continuous cooling (cooling rate of 5×10^{-2} K/ps, continuous curves; 8×80 system for PS, 64×10 system for PC), and with stepwise cooling (open squares, PS only, 1×80 chain). Straight solid lines represent the least-squares fits of data at high temperature and low temperature. The arrows indicate the simulated values of T_g obtained from the stepwise and continuous cooling for PS and from continuous cooling for PC.

change in the thermal-expansion coefficient serves as an indication of the glass transition. The regions in the vicinity of the corresponding T_g ($T_g \pm 50$ K) have been excluded from the linear fitting. The value of $T_g = 385 \pm 6$ K produced for PS by the continuous-cooling procedure is displaced towards higher temperatures as compared to the value from step-wise cooling, $T_g = 375 \pm 10$ K (performed with the order-of-magnitude slower effective cooling rate), and to the experimental value, $T_g = 373$ K [3, 12]. The simulated value of $T_g = 433 \pm 7$ K produced for PC by the continuous-cooling procedure is also displaced towards higher temperatures as compared to the experimental value of $T_g = 423$ K. If the relaxation time of the system follows a Vogel-Fulcher dependence on temperature [11], then the glass-transition temperature increases logarithmically with cooling rate; on the basis of this slow logarithmic increase realistic values of T_g are obtained by extrapolating the simulated data towards experimental cooling rates (such an extrapolation should be viewed with some caution because the scale of the available time window used for this extrapolation lies in the range of nanoseconds) [11].

Local mobility. – The differences between the two polymers as regards the local segmental mobility have been studied by measuring the mean-square translational displacements (MSTD) of individual segments, figs. 2a. As shown in [3] for PS the regime of free monomer diffusion at short times and high temperatures changes into a Rouse diffusive regime [13] with a slope of $\alpha \approx 0.5$. The same behaviour is confirmed here for PC. With decreasing temperature the motion of the chain segment is becoming more restricted: the onset of the Rouse diffusion is preceded by a crossover, or a cage effect (almost a plateau for PS), whereby very restricted motions occur in the cage formed by surrounding monomers [3]. The final parts of the MSTD curves are fitted with the power law $\langle \Delta r^2(t) \rangle = l^2 (t/\tau)^{1/2}$ ($l = 1$ Å). To remove the dependence on the choice of l, the relaxation times τ are further normalized by the value of τ at $T = 600$ K. The idealized mode-coupling theory (MCT) for the translational α-relaxation was applied in [3] for PS, and it is extended for PC in the present study. For both polymers the characteristic time algebraically diverges at some critical temperature $T_c \gtrsim T_g$: $\tau \sim (T - T_c)^{-\gamma}$, reflecting the collective behaviour of the local segmental dynamics. From the two-parameter

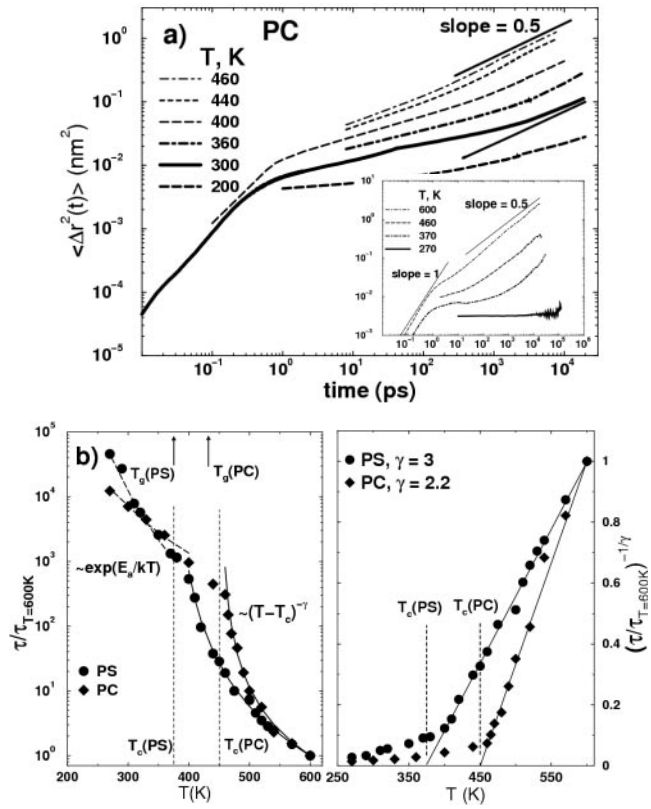

Fig. 2 – (a) MSTD of the main-chain segments of PC (64×10 system) in the vicinity of T_g. A diffusive regime with a slope close to 1 is observed up to $t = 1$ ps. An asymptotic slope of 0.5 is confirmed for temperatures close to T_g and higher. Crossover between these two regimes is a manifestation of the cage effect. Qualitatively the same behaviour is observed for PS, but the plateau between these two regimes is much more pronounced (see inset). (b) Temperature dependence of the normalized relaxation times τ for both polymers (PS, 1×80; PC, 64×10 systems). Solid lines are the MCT-based fits, dashed lines are fits with a simple activation law.

fit to the data the values of T_c and γ are extracted. For PS the value of $T_c = 375 \pm 6$ K is close to the simulated T_g, for PC the difference between $T_c = 450 \pm 2$ K and T_g is larger, see fig. 2b. We found the exponent γ to be non-universal, and equal to 3.0 ± 0.2 and 2.2 ± 0.2 for PS and PC, respectively (all error bars have been calculated using Levenberg-Marquardt least-squares fitting method). At $T < T_g$ an activated behaviour, $\tau \sim \exp[E_a/k_B T]$, is observed for the onset of the out-of-cage motion for both polymers. The activation energy for PS, $E_a = 30 \pm 2$ kJ/mol is almost twice larger than $E_a = 16.8 \pm 2$ kJ/mol for PC. The change from the ideal-MCT-like to the activated behaviour is connected to a crossover from the cooperative character of translational dynamics above T_g to individual hopping processes below T_g. For a PC melt the cage effect is far less pronounced, and the crossover appears to be more gradual. Detailed study of the α-relaxation is a subject of further investigation.

Uniaxial extension. – The main goal of the present study is to give insight through atomistic simulations into different experimental mechanical behaviour of typical amorphous polymers. Uniaxial deformation with constant deformation velocity $\dot{L} = 0.005$ Å/ps was

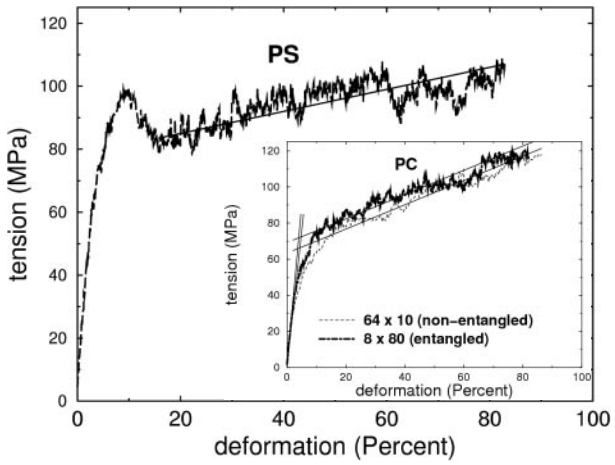

Fig. 3 – Simulated stress-strain dependence for a non-entangled model of PS (4×160 system) and two specimens of PC of different molecular weight (see inset), at $T = 300\,\mathrm{K}$. Strain softening is absent for both entangled and non-entangled PC glasses. Straight solid lines represent the least-squares fit of the data in the strain-hardening regime and elastic regime (PC only).

applied along one (X, Y or Z) of the axes to five independent sets of relaxed isotropic PS and PC samples, at different temperatures below the corresponding simulated glass transition temperatures. For the resulting fifteen different deformed samples the nominal strain parallel to the direction of deformation has been measured as $\gamma_L = \frac{L-L_0}{L_0} \times 100\%$, where $L(t) = L_0 + \dot{L}t$ is the instant length of the simulation box parallel to the direction of the applied tension and L_0 denotes the equilibrium value of this length prior to the application of tension. The results after averaging over all samples are given in fig. 3. The initial elastic regime for both polymers is clearly seen for extensions up to 3%, and is followed by the onset of the plastic flow in the so-called yield point (for PC the yield point is defined as an intersection of two tangents to the initial and final parts of the curve [4]). At $T = 300\,\mathrm{K}$ the simulated Young modulus is $2.9 \pm 0.1\,\mathrm{GPa}$ for PS and $2.2 \pm 0.2\,\mathrm{GPa}$ for PC, which is comparable to the experimental values at room temperature of 3.2–3.4 GPa and 2.34 GPa for PS and PC, respectively [12]. The simulated values of the yield stress ($100 \pm 5\,\mathrm{MPa}$ for PS and $70 \pm 5\,\mathrm{MPa}$ for PC), and the elongation at the yield point (about 7% for PS and about 5% for PC of different molecular weight) are also comparable to the experimental ones (in spite of the enormous difference in deformation rate, [14]) at the same temperature (yield stress of 95 MPa for PS and 65 MPa for PC, and elongation-at-yield of 6% for both polymers [2]).

Post-yield behaviour. – In a mechanical experiment, carried out under compression [6], a strong strain softening followed by minor hardening is observed for PS, which results in unstable post-yield deformation behaviour; in contrast PC shows less softening and more hardening, which induces toughness. After the yield point pronounced strain softening is clearly seen in fig. 3 for simulated PS, with a stress drop of about 20 MPa. Such a softening is not present for PC. For both polymers strain hardening is clearly seen at extensions above $\gamma_L = 15\%$. The strain-hardening modulus G_R is usually defined [15] as the slope of the curve at large strains (deformation above 15% in the present simulations) of the true stress σ *vs.* $\lambda^2 - \lambda^{-1}$ (neo-Hookean behaviour), $\sigma = G_R(\lambda^2 - \lambda^{-1})$, where $\lambda = \frac{L}{L_0}$. The present simulation data at $T = 300\,\mathrm{K}$ give the value $G_R = 12.0 \pm 0.5\,\mathrm{MPa}$ for PS which is almost twice lower than the simulated value of $G_R = 22 \pm 1\,\mathrm{MPa}$ for PC. These results may be compared

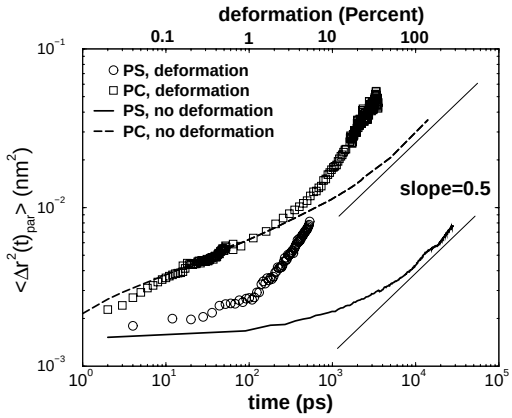

Fig. 4 – The fluctuating stochastic contributions to the parallel MSTD are shown (symbols, averaged over backbone monomers for PS and over all monomers for PC) together with the corresponding dependencies in the isotropic case (lines), 8×80 samples, $T = 300\,\mathrm{K}$. For PS the onset of the Rouse regime in the direction of the deformation starts much earlier as compared to the isotropic case. For PC the translational diffusion just after the yield point is changed less by the deformation.

with available experimental uniaxial-compression data of van Melick *et al.* [15], which give $G_R = 13\,\mathrm{MPa}$ for PS and $G_R = 29\,\mathrm{MPa}$ for PC at room temperature. In [15] the strain hardening in glassy polymers is explained by the rubber-elastic response of the entanglement network. A relatively high entanglement density for PC as compared to that for PS would lead to much higher strain hardening. The present simulations show the same strain-hardening modulus for non-entangled and entangled PC melts. We conclude here that the entanglements do not contribute to the strain hardening, at least on the simulated time scale. In [16] strain hardening is explained by a high population of the completely stretched parts of a chain in the planar configuration (trans-conformer) in deformed chains. Experimental data [15] and simulations also show a decrease in the strain hardening modulus with increasing temperature. The detailed analysis of the population of different conformers in both PS and PC as well as the influence of the cooling rate is a subject of further study.

Mobility under deformation. – Due to the uniaxial extension the mobility of the monomers will be different from that in the undeformed case. The trivial contribution to this mobility results from the constant rate of the affine extension of the sample, with a fixed velocity $\dot{L}$ at the edge. The particles throughout the sample are accordingly convected with some local velocity, which masks the polymer-specific effects of the deformation on the segmental mobility. To get rid of this trivial dependence the trajectory of each particle is modified: the local convective velocity $v_\parallel(t) = \frac{x_\parallel(t)}{L(t)}\dot{L}$ in the direction of the applied stretching is subtracted from the position of each particle $x_\parallel(t)$ in this direction, and the parallel MSTD is calculated (symbols in fig. 4). For both polymers it is clearly seen that the deformation does not influence significantly the translational mobility below the yield point (up to $t \approx 200\,\mathrm{ps}$). Changes occur in the post-yield response: for the parallel MSTD the onset of the cage escape starts just after the yield point and significantly earlier as compared to the isotropic case. For the PS glass the uniaxial mechanical deformation leads to an acceleration of the parallel diffusion by more than one order of magnitude. In the recently reported MD simulations of Capaldi *et al.* [17] for a model glassy polyethylene an increase in the *internal* dynamic behaviour, *i.e.* the dihedral-angle transition rate, has been observed under the influence of a deformation. For the PC

glass the deformation also influences the mobility, but the acceleration of the parallel diffusion is observed to be weaker as compared to PS.

We have simulated with realistic chemical detail the different bulk dynamics of two typical amorphous polymers around the glass transition together with their mobilities on the segmental level. The predictions of MCT are validated for both polymers, but with different values of the critical exponents for PS and PC. The crossover from collective to activated type of segmental relaxation is found for both polymers. The uniaxial-deformation simulations have been performed with the same deformation rate for both polymers. In spite of the difference between computational and experimental deformation rate the widely different bulk mechanical behaviour could be simulated. For PS the initial softening after the yield point is concomitant with a significant decrease of the local parallel relaxation times under deformation; this effect is less for PC as the caging is not so pronounced for this polymer. Our results give further evidence of the importance of the details of the inter- and intrachain interactions (torsions, Coulomb and excluded volume) for the different post-yield behaviour of chemically-specific polymers. Connection with the segmental orientations and differences in the cage size as well as the study of the deformation rate effects will be a subject of further investigation.

* * *

This work is part of the research program of the Dutch Polymer Institute (projects 180 and 487). Grateful acknowledgement is made to Dr. L. Govaert (TUE, Eindhoven), Prof. A. Semenov (ICS, Strasbourg) and Prof. T. Birshtein (IMC, St. Petersburg) for many useful discussions. This work was further sponsored by the Stichting Nationale Computerfaciliteiten (NCF), with financial support from the Nederlandse Organisatie voor Wetenschappelijk Onderzoek (NWO).

REFERENCES

[1] Kramer E. J. and Berger L. L., *Adv. Polym. Sci.*, **91/92** (1990) 1.
[2] Smit R. J. M., Brekelmans W. A. M. and Meijer H. E. H., *Comput. Method Appl.*, **M155** (1998) 181.
[3] Lyulin A. V., Balabaev N. K. and Michels M. A. J., *Macromolecules*, **35** (2002) 9595.
[4] Ward I. M. and Hadley D. W., *An Introduction to the Mechanical Properties of Solid Polymers* (J. Wiley and Sons, England) 1993.
[5] Callister W. D. jr. , *Materials Science and Engineering: an Introduction* (J. Wiley and Sons, Inc.) 2003.
[6] Govaert L. E., van Melick H. G. H. and Meijer H. E. H., *Polymer*, **42** (2001) 1271.
[7] van Zon A. and de Leeuw S. W., *Phys. Rev. E*, **60** (1999) 6942.
[8] Aichele M. and Baschnagel J., *Eur. Phys. J. E*, **5** (2001) 229.
[9] Hutnik M., Argon A. S. and Suter U. W., *Macromolecules*, **24** (1991) 5956.
[10] Allen M. P. and Tildesley D. J., *Computer Simulation of Liquids* (Clarendon Press, Oxford) 1987.
[11] Lyulin A. V., Balabaev N. K. and Michels M. A. J., *Macromolecules*, **36** (2003) 8574.
[12] Mark James E. (Editor), *Polymer Data Handbook* (Oxford University Press, Oxford) 1999.
[13] Doi M. and Edwards S. F., *The Theory of Polymer Dynamics* (Clarendon Press, Oxford) 1986.
[14] Rottler J. and Robbins M. O., *Phys. Rev. E*, **68** (2003) 011507.
[15] van Melick H. G. H., Govaert L. E. and Meijer H. E. H., *Polymer*, **44** (2003) 2493.
[16] McKechnie J. I., Haward R. N., Brown D. and Clarke J. H. R., *Macromolecules*, **26** (1993) 198.
[17] Capaldi F. M., Boyce M. C. and Rutledge G. C., *Phys. Rev. Lett.*, **89** (2002) 175505.